Available online at www.sciencedirect.com
SCIENCE DIRECT
International Journal of Heat and Mass Transfer 49 (2006) 763–769
International Journal of HEAT and MASS TRANSFER
www.elsevier.com/locate/ijhmt

Self-similar solidification of an alloy from a cooled boundary

D.V. Alexandrov *, A.P. Malygin

Department of Mathematical Physics, Urals State University, Lenin Avenue 51, Ekaterinburg 620083, Russia

Received 1 February 2005; received in revised form 14 June 2005
Available online 7 October 2005

Abstract

The self-similar solidification process of an alloy from a cooled boundary is studied on the basis of two models with a planar front and mushy layer. Approximate and exact analytical solutions of the process, which demonstrate unusual dynamics near the point of constitutional supercooling, are found. The rate of solidification and front position of the solid/mush boundary (parabolic growth rate constant) are expressed in an explicit form in the case of slow dynamics of this boundary. The theory under consideration is in a good agreement with experimental and numerical studies carried out by Huppert and Worster for ice growing from aqueous salt solutions.

Keywords: Solidification; Mushy region; Solid–liquid transitions

1. Introduction

Some types of instabilities of the phase interface and the instability of the metastable constitutionally supercooled binary melt cause a system of elements of the solid phase in the form of dendrites, cells and others to appear in the melt. The development of this system reduces the supercooling and leads to formation of a new stable solidification mode characterized by the presence of a mushy layer that separates the pure solid and melt regions. Heat and mass transfer in the mushy layer has a major effect on the properties of the solid materials thus produced, which is also responsible for the marked interest in the study of solidification of binary melts accompanied by formation of the aforementioned transition layer. Mathematical descriptions of solidification scenario are complicated not only by nonlinearities of heat and mass transfer equations but also by the need to apply boundary conditions at solid/liquid interfaces which are evolving with time and whose positions must be determined as a part of the solution. A full set of thermodynamic equations for a mushy layer is developed and a much-reduced set of them is solved approximately in Ref. [1] for the constrained growth of a binary alloy. More complete and exact solutions have since been given in Refs. [2–5]. Constrained growth, in which the interfaces are supposed to advance at a prescribed constant velocity, is applicable to industrial crystal pulling (Czochralski growth), but not to the solidification of castings nor to many natural systems where growth can proceed at a rate dependent on time and, in particular, at a rate inversely proportional to the square root of time [6,7]. The aim of this paper is to develop the theory where the interfaces propagate in this manner.

2. Self-similar solidification with a planar front

We treat a unidirectional solidification of a binary melt along z-axis from a cooled boundary experimentally and numerically studied in Refs. [6,7]. Let us consider a semi-infinite region $z > 0$ filled with liquid which initially has uniform composition $C = c_0$ and temperature T_∞. We traditionally neglect the solute transport in the solid phase and, following Ref. [7], ignore the effects of gravity and imagine that the plane $z = 0$ forms the lower, horizontal boundary of the domain. The temperature of the cooled boundary is maintained at a value $T = T_B$ lower than the initial liquidus temperature. The temperature T and

* Corresponding author. Tel.: +7 343 3 507541; fax: +7 343 3 507401.
E-mail address: Dmitri.Alexandrov@usu.ru (D.V. Alexandrov).

0017-9310/$ - see front matter
doi:10.1016/j.ijheatmasstransfer.2005.07.047

Nomenclature

a	solid/mush interface position
b	mush/liquid interface position
c_0	solute concentration at infinity
C	solute concentration
C_{pl}	specific heat of the liquid phase
C_{ps}	specific heat of the solid phase
D	solute diffusivity
h	front position
k_{l}	thermal conductivity of the liquid phase
k_{s}	thermal conductivity of the solid phase
L	latent heat parameter
t	time
T	temperature
T_{B}	temperature at $z = 0$
T_∞	temperature at infinity
z	spatial coordinate

Greek symbols

Γ	liquidus slope
η	self-similar coordinate
λ, λ_a, λ_b	parabolic growth rate constants
ρ_{l}	density of the liquid phase
ρ_{s}	density of the solid phase
φ	local volume fraction of the solid phase
χ	local volume fraction of the liquid phase

concentration C fields in the solid and liquid phases are described by the classical heat and mass transfer equations:

$$\rho_{\mathrm{s}} C_{\mathrm{ps}} \frac{\partial T}{\partial t} = k_{\mathrm{s}} \frac{\partial^2 T}{\partial z^2}, \quad 0 < z < h(t), \tag{1}$$

$$\rho_{\mathrm{l}} C_{\mathrm{pl}} \frac{\partial T}{\partial t} = k_{\mathrm{l}} \frac{\partial^2 T}{\partial z^2}, \qquad \frac{\partial C}{\partial t} = D \frac{\partial^2 C}{\partial z^2}, \quad z > h(t), \tag{2}$$

where $z = h(t)$ is the position of the solidification front; all of the transfer coefficients are assumed to be constant in each phase. In the case of unidirectional regime with a planar front, nothing depends on the spatial coordinate directed perpendicular to the solidification direction.

The aforementioned boundary conditions can be expressed in the form

$$T = T_{\mathrm{B}}, \quad z = 0, \tag{3}$$

$$C \to c_0, \quad T \to T_\infty, \quad z \to \infty. \tag{4}$$

Further, we make the assumption that the front, $z = h(t)$, is close to equilibrium, that is,

$$T(h,t) = -\Gamma C(h^+, t), \; z = h(t). \tag{5}$$

Heat and solute must be conserved at the front

$$\rho_{\mathrm{s}} L \frac{\mathrm{d}h}{\mathrm{d}t} = k_{\mathrm{s}} \left(\frac{\partial T}{\partial z}\right)_{z=h^-} - k_{\mathrm{l}} \left(\frac{\partial T}{\partial z}\right)_{z=h^+}, \tag{6}$$

$$C(h^+, t) \frac{\mathrm{d}h}{\mathrm{d}t} + D \left(\frac{\partial C}{\partial z}\right)_{z=h^+} = 0. \tag{7}$$

The aforementioned model (1)–(7) admits a similarity solution with variable η and interface position $h(t)$ of the form

$$\eta = \frac{z}{\sqrt{4Dt + s}}, \quad h(t) = \lambda \sqrt{4Dt + s}, \tag{8}$$

where the parabolic growth rate constant λ is to be determined and s has the meaning $h^2(0)/\lambda^2$.

In a similarity solution a similarity variable, combining the space and time variables, is sought that transforms the governing partial differential equations into a set of ordinary differential equations with the similarity variable as the independent variable.

Following the presentation of Ref. [7] and omitting mathematical manipulations, let us express the solution of the above model using self-similar variables (8). The result is

$$T(\eta) = T_{\mathrm{B}} + \frac{(T_h - T_{\mathrm{B}})\mathrm{erf}(\varepsilon_{\mathrm{s}}\eta)}{\mathrm{erf}(\varepsilon_{\mathrm{s}}\lambda)}, \quad \eta < \lambda, \tag{9}$$

$$T(\eta) = T_\infty + \frac{(T_h - T_\infty)\mathrm{erfc}(\varepsilon_{\mathrm{l}}\eta)}{\mathrm{erfc}(\varepsilon_{\mathrm{l}}\lambda)}, \quad \eta > \lambda, \tag{10}$$

$$C(\eta) = c_0 + \frac{(C_h - c_0)\mathrm{erfc}(\eta)}{\mathrm{erfc}(\lambda)}, \quad \eta > \lambda, \tag{11}$$

where $\varepsilon_{\mathrm{s}} = \sqrt{DC_{\mathrm{ps}}\rho_{\mathrm{s}}/k_{\mathrm{s}}}$, $\varepsilon_{\mathrm{l}} = \sqrt{DC_{\mathrm{pl}}\rho_{\mathrm{l}}/k_{\mathrm{l}}}$, T_h and C_h stand for the temperature and concentration at the phase transition boundary $\eta = \lambda$. Three unknowns are determined by the boundary conditions (5)–(7). Substituting distributions (9)–(11) in conditions (5)–(7), we arrive at

$$T_h = -\Gamma C_h, \quad C_h - c_0 = C_{\mathrm{fi}}(\lambda) \equiv \frac{c_0 F(\lambda)}{1 - F(\lambda)}, \tag{12}$$

$$\Gamma C_{\mathrm{fi}}(\lambda) \left[\frac{\beta}{F(\varepsilon_{\mathrm{l}}\lambda)} + \frac{1}{G(\varepsilon_{\mathrm{s}}\lambda)}\right] = \frac{T_1}{G(\varepsilon_{\mathrm{s}}\lambda)} - \frac{\beta T_0}{F(\varepsilon_{\mathrm{l}}\lambda)} - \frac{L}{C_{\mathrm{ps}}}, \tag{13}$$

where

$$\beta = \frac{\rho_{\mathrm{l}} C_{\mathrm{pl}}}{\rho_{\mathrm{s}} C_{\mathrm{ps}}}, \quad F(x) = \sqrt{\pi} x \exp(x^2)\mathrm{erfc}(x),$$

$$G(x) = \sqrt{\pi} x \exp(x^2)\mathrm{erf}(x).$$

Eq. (13) determines the parabolic growth rate constant. The driving temperature differences $T_1 = -\Gamma c_0 - T_{\mathrm{B}}$ and $T_0 = T_\infty + \Gamma c_0$ and graphs of λ versus T_1, T_0 and c_0 are shown in the many figures of Ref. [7].

It is noteworthy that the temperature ahead of the plane solidification front can fall below the local liquidus temperature. This phenomena is called "constitutional supercooling". The latter arises if the concentration gradient exceeds the temperature one at the front, i.e.

$$\left(\frac{\partial T}{\partial z}\right)_{z=h^+} < -\Gamma\left(\frac{\partial C}{\partial z}\right)_{z=h^+}. \tag{14}$$

Now, substituting distributions (10) and (11) in inequality (14), taking into consideration definition (12), we rewrite the last condition for the self-similar solidification front

$$C_{\mathrm{fi}}(\lambda) > C_i(\lambda) \equiv \frac{(T_0/\Gamma)\varepsilon_1^2 F(\lambda)}{F(\varepsilon_1\lambda) - \varepsilon_1^2 F(\lambda)}. \tag{15}$$

If the left hand side of (15) is equal to the right one, the last condition determines the onset of supercooling and, consequently, critical values of thermophysical parameters that describe the validity of the above solutions for the planar front. Therefore, if inequality (15) holds true, we shall use a mushy layer model.

3. Self-similar solidification with a mushy layer

Let us analyze the solidification of a binary melt with a mushy layer, in which heterogeneous inclusions of the new phase grow in such a manner that this layer is virtually totally desupercooled. In this case, a mushy layer may be treated as independent of the precise morphology of the growing solid phase. The mush is also treated as a continuum, and its physical properties are taken to be functions of the local volume fraction of solid φ. Heat and mass transfer are described by heat conduction and diffusion equations in the mushy layer ($a(t)$ and $b(t)$ stand for the solid/mush and mush/liquid boundaries)

$$(\rho C_p)_{\mathrm{m}}\frac{\partial T}{\partial t} = \frac{\partial}{\partial z}\left(k_{\mathrm{m}}\frac{\partial T}{\partial z}\right) + \rho_{\mathrm{s}} L\frac{\partial \varphi}{\partial t},$$
$$T = -\Gamma C, \quad a(t) < z < b(t), \tag{16}$$
$$\chi\frac{\partial C}{\partial t} = \frac{\partial}{\partial z}\left(D\chi\frac{\partial C}{\partial z}\right) + C\frac{\partial \varphi}{\partial t},$$
$$\chi = 1-\varphi, \quad a(t) < z < b(t), \tag{17}$$

where the thermal properties (k_{m} and $(\rho C_p)_{\mathrm{m}}$) of the mush are assumed to be volume-fraction-weighted averages of the properties of the individual phases so that [8]

$$k_{\mathrm{m}} = \chi k_{\mathrm{l}} + (1-\chi)k_{\mathrm{s}}, \quad (\rho C_p)_{\mathrm{m}} = \chi\rho_{\mathrm{l}}C_{\mathrm{pl}} + (1-\chi)\rho_{\mathrm{s}}C_{\mathrm{ps}}.$$

Let us especially emphasize that there is no reason for φ to be continuous in the model under consideration [7].

The heat and mass flux conditions imposed at the two interfaces have the form

$$\rho_{\mathrm{s}} L\chi_a\frac{\mathrm{d}a}{\mathrm{d}t} = k_{\mathrm{s}}\left(\frac{\partial T}{\partial z}\right)_{z=a^-} - k_{\mathrm{m}}\left(\frac{\partial T}{\partial z}\right)_{z=a^+},$$
$$C_a\chi_a\frac{\mathrm{d}a}{\mathrm{d}t} = -D\chi_a\left(\frac{\partial C}{\partial z}\right)_{z=a^+},$$
$$\rho_{\mathrm{s}} L(1-\chi_b)\frac{\mathrm{d}b}{\mathrm{d}t} = k_{\mathrm{m}}\left(\frac{\partial T}{\partial z}\right)_{z=b^-} - k_{\mathrm{l}}\left(\frac{\partial T}{\partial z}\right)_{z=b^+},$$
$$C_b(1-\chi_b)\frac{\mathrm{d}b}{\mathrm{d}t} = D\chi_b\left(\frac{\partial C}{\partial z}\right)_{z=b^-} - D\left(\frac{\partial C}{\partial z}\right)_{z=b^+}. \tag{18}$$

As is shown in Ref. [7], the traditional approximation $\chi_b = 1$ ($\varphi_b = 0$) is unjustifiable a priori. Further, we have a condition of marginal equilibrium of the liquid [9]

$$\left(\frac{\partial T}{\partial z}\right)_{z=b^+} = -\Gamma\left(\frac{\partial C}{\partial z}\right)_{z=b^+}. \tag{19}$$

The last boundary condition shows that none of the liquid region is supersaturated, and it is marginal in the sense that (19) gives the smallest temperature gradient consistent with complete equilibrium, cf. (14). The possibility of using a condition of marginal stability is also discussed in Ref. [7].

The governing equations (16) and (17) supplemented by the boundary conditions (18) and (19) admit similarity solutions with the same similarity variable η and interface positions of the form

$$a(t) = \lambda_a\sqrt{4Dt+s}, \quad b(t) = \lambda_b\sqrt{4Dt+s}, \tag{20}$$

where λ_a and λ_b are parabolic growth rate constants determined below.

Rewriting the governing equations (16) and (17) and the boundary conditions (18) and (19) in terms of self-similar variables (8) and (20), eliminating the temperature field, we come to the following model

$$-2\eta(1-\varphi)\frac{\mathrm{d}C}{\mathrm{d}\eta} = -\frac{\mathrm{d}\varphi}{\mathrm{d}\eta}\frac{\mathrm{d}C}{\mathrm{d}\eta} + (1-\varphi)\frac{\mathrm{d}^2C}{\mathrm{d}\eta^2} - 2\eta C\frac{\mathrm{d}\varphi}{\mathrm{d}\eta},$$
$$\alpha = \frac{\Gamma C_{\mathrm{ps}}}{L}, \quad \lambda_a < \eta < \lambda_b, \tag{21}$$
$$-2\alpha\varepsilon_{\mathrm{s}}^2[\beta + (1-\beta)\varphi]\eta\frac{\mathrm{d}C}{\mathrm{d}\eta} = [\Lambda + (1-\Lambda)\varphi]\alpha\frac{\mathrm{d}^2C}{\mathrm{d}\eta^2} + \alpha(1-\Lambda)\frac{\mathrm{d}\varphi}{\mathrm{d}\eta}\frac{\mathrm{d}C}{\mathrm{d}\eta} + 2\varepsilon_{\mathrm{s}}^2\eta\frac{\mathrm{d}\varphi}{\mathrm{d}\eta},$$
$$\Lambda = \frac{k_{\mathrm{l}}}{k_{\mathrm{s}}}, \quad \lambda_a < \eta < \lambda_b, \tag{22}$$
$$C = c_0 + C_i(\lambda_b), \quad \eta = \lambda_b, \tag{23}$$
$$\left[\frac{\varepsilon_{\mathrm{s}}^2\chi_b}{\alpha} + \frac{k_{\mathrm{m}}(\chi_b)}{k_{\mathrm{s}}}C_b - \frac{C_i(\lambda_b)}{F(\lambda_b)}\right](1-\chi_b) = 0,$$
$$\eta = \lambda_b, \tag{24}$$
$$\frac{\mathrm{d}C}{\mathrm{d}\eta} = -2\lambda_b\left[\frac{k_{\mathrm{l}}}{k_{\mathrm{m}}(\chi_b)}\frac{C_i(\lambda_b)}{F(\lambda_b)} + \frac{\varepsilon_{\mathrm{s}}^2}{\alpha}\frac{k_{\mathrm{s}}}{k_{\mathrm{m}}(\lambda_b)}(1-\chi_b)\right],$$
$$\eta = \lambda_b, \tag{25}$$
$$\left[2\lambda_a\frac{\varepsilon_{\mathrm{s}}^2}{\alpha}\chi_a - \frac{k_{\mathrm{m}}(\chi_a)}{k_{\mathrm{s}}}\frac{\mathrm{d}C}{\mathrm{d}\eta}\right]G(\varepsilon_{\mathrm{s}}\lambda_a) + 2\lambda_a\varepsilon_{\mathrm{s}}^2\left[C + \frac{T_{\mathrm{B}}}{\Gamma}\right] = 0,$$
$$\eta = \lambda_a, \tag{26}$$
$$\left[\frac{\mathrm{d}C}{\mathrm{d}\eta} + 2\lambda_a C\right]\chi_a = 0, \quad \eta = \lambda_a. \tag{27}$$

The heat and mass transfer equations (21) and (22) with boundary conditions (23)–(27) form a closed model describing a mushy layer.

The boundary condition (23) is analogous to condition (12). This condition may be easily obtained by means of expressions (15) and (19). The boundary condition (24) derived in Ref. [7] from a condition of marginal equilibrium represents a quadratic equation for the liquid fraction χ_b at the mush/liquid interface. It is clearly seen that one of the roots is $\chi_b = 1$ (the boundary condition traditionally used by many authors; see, among others, [1,4,5]). However, it was shown [7] that the other root is

$$\chi_b = \chi_i \equiv \frac{c_0[C_i(\lambda_b)/C_{\mathrm{fi}}(\lambda_b) - 1]}{\varepsilon_s^2/\alpha + C_b(k_1/k_s - 1)}. \tag{28}$$

In other words, we choose as our boundary condition $\chi_b = \chi_i$ if $0 \leqslant \chi_i < 1$ and $\chi_b = 1$ otherwise [7]. The boundary condition (27) must be treated in the same manner. The possible changeover of these boundary conditions will also be discussed subsequently.

4. Approximate solutions

Analytical studies of relationships governing solidification in the presence of a non-stationary mushy layer is extremely complicated. This happens because it is necessary to investigate the interaction of nonlinear heat and mass transfer and phase transitions at both interfaces. Therefore, many of the classical models were analyzed by numerical methods only, which do not allow establishing clear relationships between the state variables of the process and the characteristics of the structure of the mushy region. This situation stimulates the search of new, unconventional approaches to solving the solidification problems with a mushy layer. One of such constructive approaches developed here is adopted for self-similar solidification scenaria with a mushy layer. Our approach consists in the following.

Let us seek the solutions of the above model in the form of series in η

$$\begin{aligned} \varphi(\eta) &= \varphi_0 + \eta\varphi_1 + \eta^2\varphi_2 + \cdots, \\ C(\eta) &= C_0 + \eta C_1 + \eta^2 C_2 + \eta^3 C_3 + \cdots, \end{aligned} \tag{29}$$

where the coefficients φ_i and C_i are independent on the self-similar variable. Substituting expansions (29) into Eqs. (21) and (22), we find two equations in the zero approximation in η

$$\begin{aligned} &\varphi_1 C_1 = 2(1-\varphi_0)C_2, \\ &2C_2[\Lambda + (1-\Lambda)\varphi_0] + (1-\Lambda)\varphi_1 C_1 = 0. \end{aligned}$$

The solution of these equations determines coefficients φ_1 and C_2 such that $\varphi_1 = 0$ and $C_2 = 0$. Further, we obtain the following expressions for first-order terms with respect to η. In terms of φ_2 and C_3 they are

$$\begin{aligned} &\varphi_2 = (1-\varphi_0)\left[\Lambda + (1-\Lambda)\varphi_0 - \varepsilon_s^2(\beta + (1-\beta)\varphi_0)\right], \\ &C_3 = L_0(\lambda_b)C_1, \\ &L_0(\lambda_b) = -\frac{(1-\Lambda)(1-\varphi_0) + \varepsilon_s^2[\beta + (1-\beta)\varphi_0]}{3}. \end{aligned} \tag{30}$$

Now, substituting (30) in the boundary condition $\varphi(\lambda_b) = \varphi_b = \varphi_0 + \lambda_b^2\varphi_2$, we arrive at a quadratic equation for $\varphi_0(\lambda_b)$

$$\begin{aligned} \varphi_0(\lambda_b) &= \varphi_0^- = \frac{-b_1 - \sqrt{b_1^2 - 4a_1c_1}}{2a_1}, \\ \varphi_0(\lambda_b) &= \varphi_0^+ = \frac{-b_1 + \sqrt{b_1^2 - 4a_1c_1}}{2a_1}, \end{aligned} \tag{31}$$

where

$$\begin{aligned} &a_1(\lambda_b) = \lambda_b^2[1 - \Lambda - \varepsilon_s^2(1-\beta)], \\ &b_1(\lambda_b) = [2\Lambda\lambda_b^2 - \lambda_b^2 - 1 + \varepsilon_s^2\lambda_b^2(1-2\beta)], \\ &c_1(\lambda_b) = \varphi_b(\lambda_b) - \lambda_b^2(\Lambda - \varepsilon_s^2\beta), \\ &\varphi_b(\lambda_b) = 1 - \chi_b(\lambda_b). \end{aligned}$$

The boundary condition (23) gives

$$C_0(\lambda_b) = c_0 + C_i(\lambda_b) - \lambda_b C_1[1 + \lambda_b^2 L_0(\lambda_b)]. \tag{32}$$

The value of C_1 is found from the boundary condition (27). Let $\chi_a \neq 0$ then we have from (27)

$$C_1 = -\frac{2\lambda_a[c_0 + C_i(\lambda_b)]}{1 + 2\lambda_a^2 - 2\lambda_a\lambda_b + L_0(\lambda_b)[3\lambda_a^2 + 2\lambda_a^4 - 2\lambda_a\lambda_b^3]}. \tag{33}$$

Substituting the second of expansions (29) into the boundary condition (25), we express C_1 in the form

$$\begin{aligned} &C_1(\lambda_b) = H_1(\lambda_b), \quad H_1(\lambda_b) = -\frac{H(\lambda_b)}{k_m(\lambda_b)[1 + 3\lambda_b^2 L_0(\lambda_b)]}, \\ &H(\lambda_b) = 2\lambda_b\left[k_1\frac{C_i(\lambda_b)}{F(\lambda_b)} + \frac{\varepsilon_s^2 k_s}{\alpha}(1-\chi_b)\right]. \end{aligned} \tag{34}$$

Combining the above solutions and the boundary condition (26), we come to the transcendential equation of the form

$$\begin{aligned} &\left[2\lambda_a\frac{\varepsilon_s^2}{\alpha}\chi_a - \frac{k_m(\chi_a)}{k_s}\left(C_1 + 3\lambda_a^2 C_3\right)\right]G(\varepsilon_s\lambda_a) \\ &\quad + 2\lambda_a\varepsilon_s^2\left[C_0 + \lambda_a C_1 + \lambda_a^3 C_3 + \frac{T_B}{\Gamma}\right] = 0. \end{aligned} \tag{35}$$

The roots of Eqs. (34) and (35) determine the parabolic growth rate constants λ_a and λ_b as functions of all thermophysical parameters of the process under consideration.

In the case of $\lambda_a \ll \lambda_b$, it is possible to express λ_a in an explicit form. To do it let us equate C_1 from (33) and (34). As a result, we come to a quadratic equation for the interface position λ_a, which gives

$$\begin{aligned} &\lambda_a(\lambda_b) = \frac{-r_2 \pm \sqrt{r_2^2 - 4r_1H_1}}{2r_1}, \\ &r_1(\lambda_b) = H_1(\lambda_b)(2 + 3L_0(\lambda_b)), \\ &r_2(\lambda_b) = 2[c_0 + C_i(\lambda_b)] - 2H_1(\lambda_b)\lambda_b(1 + \lambda_b^2 L_0(\lambda_b)). \end{aligned} \tag{36}$$

Our computations show that the solution can be found if the plus sign is chosen in the above expression. In this case,

we have only one nonlinear equation (35) for the parabolic growth rate constant λ_b.

In the case of $\varphi_a = 1$ (or $\chi_a = 0$) the boundary condition following from (27) of the form $dC/d\eta + 2\lambda_a C = 0$ at $\eta = \lambda_a$ is absent. The coefficients φ_2, C_3, φ_0, C_0 and C_1 are determined as before by formulas (30), (31), (32) and (34) respectively, whereas the parabolic growth rate constant λ_a is found from condition $\varphi_0(\lambda_b) + \lambda_a^2\varphi_2(\lambda_b) = 1$. Thus, if this is really the case, we have

$$\lambda_a(\lambda_b) = \sqrt{\frac{1-\varphi_0(\lambda_b)}{\varphi_2(\lambda_b)}}, \tag{37}$$

whereas λ_b is found from (35).

Thus, the approximate solution of the problem under consideration is described by expressions (24) and (29)–(37).

We restrict ourselves by the set of thermophysical parameters given in Table 1. Now we present results for a solution of sodium nitrate in water, where the concentration measures the weight per cent of $NaNO_3$. Fig. 1 shows the parabolic growth rate constants and the volume fractions of solid as functions of T_1. It is easy to see that the approximate solutions are in a good agreement with numerical and experimental studies of Refs. [6,7]. Fig. 2 demonstrates similar results to those in Fig. 1 in the vicinity of the critical point. As is seen, in this case, we have so-called subcritical bifurcation so that equilibrium solutions

Table 1
Parameter values for the set $NaNO_3 + H_2O$ used in calculations [7]

Property	Value	Units
Γ	0.4	°C
L	3.35×10^5	J kg^{-1}
D	10^{-9}	m^2 s^{-1}
k_s	2.219	J m^{-1} s^{-1} °C^{-1}
k_l	0.544	J m^{-1} s^{-1} °C^{-1}
ρ_s	920	kg m^{-3}
ρ_l	1000	kg m^{-3}
C_{ps}	2.01×10^3	J kg^{-1} °C^{-1}
C_{pl}	4.187×10^3	J kg^{-1} °C^{-1}

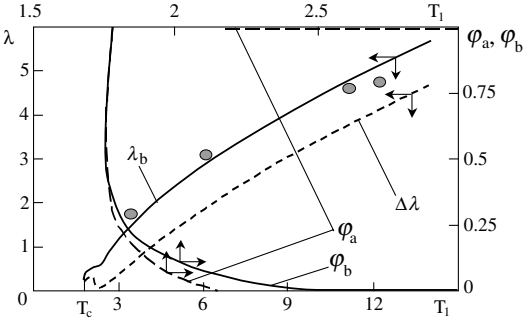

Fig. 1. The dimensionless parabolic growth rate constants λ, λ_b, the mushy layer thickness $\Delta\lambda = \lambda_b - \lambda_a$ and the volume fractions of solid φ_a and φ_b as functions of T_1 for the parameter values given in Table 1, $T_\infty = 15$ °C, $c_0 = 14$ (supercooling occurs in the liquid at $T_1 = 1.776$ and $\lambda = \lambda_b = 0.154$). The circles are data from the experiments of Ref. [6].

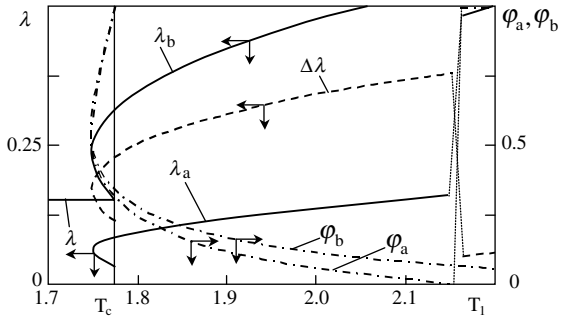

Fig. 2. An enlargement of the subcritical bifurcation in Fig. 1. The vertical dashed lines show the jumps in λ_a, $\Delta\lambda$ and φ_a at a certain value of $T_1 = T_{c1}$ (see also Fig. 4).

for the solidification regime with a mushy layer are existed for values of T_1 less than the critical value for supercooling calculated by equating both sides of inequality (15) to each other (supercooling occurs ahead of the planar front if $T_1 > T_c = 1.776$ and $\lambda > 0.154$). The solid fraction distributed within the mushy layer and the scheme of solidification are plotted in Figs. 3 and 4. As is demonstrated in Figs. 1–4, in the vicinity of the critical point, ($T_1 = T_c$, $\lambda = \lambda_b$), the solid fraction is large throughout the mush

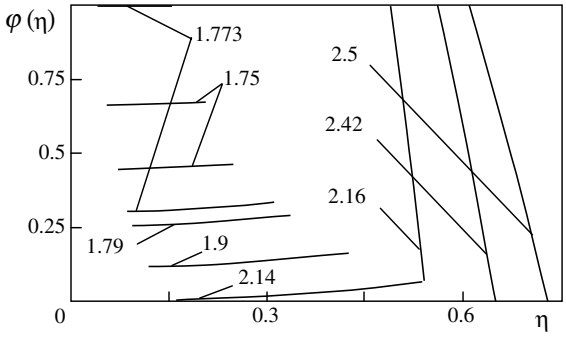

Fig. 3. Profiles of the volume fraction of solid within the mushy layer $\lambda_a < \eta < \lambda_b$ for different values of T_1 (numbers at the curves). Variations of T_1 between 2.14 and 2.16 °C gives different behavior of $\varphi(\eta)$.

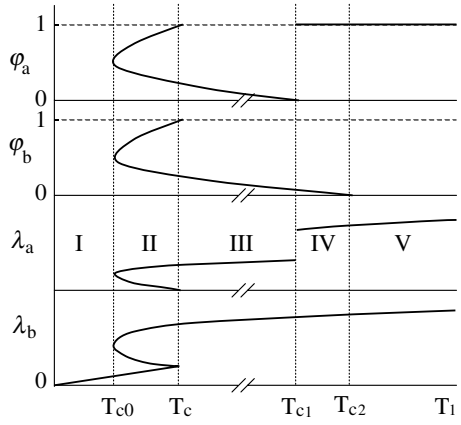

Fig. 4. Schematic diagram of solidification illustrating different behavior of the process for various values of T_1.

Table 2
Changeover of the boundary conditions for different regimes shown in Fig. 4

Planar front	I	(9)–(13)
Planar front or mushy layer	II	Planar front: same as in region I Mushy layer: same as in region III
	III	$\varphi_b \neq 0$, $\varphi_a \neq 1$, φ_0^-
Mushy layer	IV	$\varphi_b \neq 0$, $\varphi_a = 1$, φ_0^+
	V	$\varphi_b = 0$, $\varphi_a = 1$, φ_0^+

and, in particular φ_a, φ_b and $\varphi(\eta)$ approach to unity at this point. This circumstance permits us to suggest the formation of cells (possibly deep cells) rather than dendrites and other formations in this case (an example of such a behavior is illustrated in Fig. 11 of Ref. [7]; see also discussions given by Worster [7]). The subcritical bifurcation shows that three branches of the solution (one branch of λ with a planar front and two branches of λ_b with a mush) may exist in the open interval $T_{c0} < T_1 < T_c$ (see Figs. 4 and 2). Notice that the curve for λ_a does not join with the critical point. Increasing T_1 from T_c to T_{c1}, we see that the volume fraction φ_a decreases to 0 at point T_{c1} and attains unity like the step function. This a switch point when the boundary condition $dC/d\eta + 2\lambda_a C = 0$ at $\eta = \lambda_a$ must be replaced by condition $\chi_a = 0$ (see (27)). In a small vicinity of this point, the system can make no distinction between two possible regimes with $\varphi_a \neq 1$ and $\varphi_a = 1$. In other words, the system near the critical point T_{c1} tends to one of these solidification scenarios (Figs. 1, 2 and 4). Thereafter, the volume fraction φ_b attains its minimal value at point $T_1 = T_{c2}$, i.e. $\varphi_b = 0$ for $T_1 \geqslant T_{c2}$ (traditionally used boundary condition for φ_b [1,4,5]). As a consequence, instead of the boundary condition $\chi_b = \chi_i$ we have $\chi_b = 1$ at $\eta = \lambda_b$ (see (24)). Table 2 shows the detailed boundary conditions applicable for the calculated regions in Fig. 4. This example demonstrates unconventional behavior of the system near the critical points.

5. Exact analytical solutions: deep cells

The main objective of this section is to show how the deep cells or cracks ($\lambda_a = 0$) in solids can be formed in principle due to the influence of constitutional supercooling. For this purpose, we demonstrate here that the governing equations for a mush have a particular solution. Let us consider the case of $\varphi(\eta) \to 1$ ($d\varphi/d\eta \to 0$) within the mushy layer. Such a situation describes deep cells or cracks with small cross-sections filled with the liquid [7]. It is easily seen, that Eq. (21) and the boundary conditions (24), (26) and (27) are satisfied automatically whereas Eq. (22) leads to

$$\frac{d^2C}{d\eta^2} = -2\varepsilon_s^2\eta\frac{dC}{d\eta}.$$

Integration gives

$$C(\eta) = A\int_{\lambda_b}^{\eta}\exp(-\varepsilon_s^2 z^2)dz + B. \tag{38}$$

Thus, the mushy layer model under study can be solved exactly. Once a crack or deep cell has been formed in the solid, the process can be described by a mushy layer model. However, such a layer is far from equilibrium and, consequently, it cannot be described by the equilibrium model under consideration. At the beginning (as long as the fluid flowing into a crack), the mushy zone is essentially unsteady state and, therefore, we can apply the boundary conditions (23) and (25) at a later time only. In this case, we have

$$A = -2\lambda_b\exp(\varepsilon_s^2\lambda_b)\left[\frac{k_l}{k_s}\frac{C_i(\lambda_b)}{F(\lambda_b)} + \gamma\varepsilon_s^2\right],$$
$$B = c_0 + C_i(\lambda_b). \tag{39}$$

It is significant that the parabolic growth rate constant in Eq. (39) is found from equality $C_i(\lambda_b) = C_{fi}(\lambda_b)$ that follows from Eq. (28). In other words, at the instant the constitutional supercooling occurs (inequality (15) reduces to equality), the deep cells or cracks in solids can be formed (this is caused, for example, due to the fact that the ice density at the phase transition interface increases with decreasing the phase transition temperature and, as a consequence, mechanical tensions in the solid may appear). Comparing this result with Fig. 4 we conclude that three different regimes can be realized in the vicinity of the critical point T_c: planar front and mushy layer with $\lambda_a \neq 0$ (formation of cells, Fig. 4) and $\lambda_a = 0$ (formation of deep cells). In other words, it is a bifurcation type point. Of course, such phenomena as natural convection or time variations of temperature T_B must be taken into account in practice (for example, formation of sea ices occurs upon atmospheric temperature variations and convective motions [10,11]). Nevertheless, as is shown, one of the possible mechanisms of this process consists in the role of constitutional supercooling.

6. Concluding remarks

The model equations for a mush in the case of self-similar solidification regime are solved approximately by means of power expansion method. The obtained solutions accurately describe existing experimental observations and numerical simulations carried out by Huppert and Worster [6,7]. One particular (exact) solution, which corresponds to the solidification with deep cells or cracks forming a mushy layer, is revealed. It was shown that three different crystallization regimes may exist near the point of constitutional supercooling (one regime with a planar front and two mushy layer regimes with rather shallow and deep cells). Generally speaking, the self-similar solidification scenario does not closely correspond to natural conditions of sea ice formation because the atmospheric temperature at the ice surface is a function of time (in reality, the natural convection and other processes are of importance as well) [10,11]. This leads to variations in temperature T_B (e.g., according to experimental data in

Ref. [10]), which destroy the self-similar regime under consideration and cause a non-stationary solidification where the rate is not inversely proportional to the square root of time. Nevertheless, the present study shows a possibility of the formation of deep cells and cracks due to the effect of constitutional supercooling although other processes can be greater intensive than the latter. To appreciate the significance of this phenomenon, it is required to study the dynamics of fully non-stationary solidification where the rate is not inversely proportional to the square root of time in advance.

Acknowledgement

This work was made possible in part by Award No. REC-005 (EK-005-X1) of the US Civilian Research and Development Foundation for the Independent States of the Former Soviet Union (CRDF) and due to the financial support of grants Nos. 05-01-00240, 04-02-96002 Ural, 04-01-96008 Ural (Russian Foundation for Basic Research). One of the authors, D. Alexandrov, is grateful to BRHE program (CRDF and Minobrazovanie RF, grant no. Y1-PME-05-02).

References

[1] R.N. Hills, D.E. Loper, P.H. Roberts, A thermodynamically consistent model of a mushy zone, Q. J. Appl. Math. 36 (1983) 505–539.
[2] A.C. Fowler, The formation of freckles in binary alloys, IMA J. Appl. Math. 35 (1985) 159–174.
[3] Yu.A. Buyevich, L.Yu. Iskakova, V.V. Mansurov, The nonlinear dynamics of solidification of a binary melt with a quasi-equilibrium mushy region, Can. J. Phys. 68 (1990) 790–793.
[4] D.V. Alexandrov, Solidification with a quasiequilibrium mushy region: exact analytical solution of nonlinear model, J. Crystal Growth 222 (2001) 816–821.
[5] D.V. Alexandrov, Solidification with a quasiequilibrium two-phase zone, Acta Mater. 49 (2001) 759–764.
[6] H.E. Huppert, M.G. Worster, Dynamic solidification of a binary melt, Nature 314 (1985) 703–707.
[7] M.G. Worster, Solidification of an alloy from a cooled boundary, J. Fluid Mech. 167 (1986) 481–501.
[8] G.K. Batchelor, Transport properties of two-phase materials with random structure, Ann. Rev. Fluid Mech. 6 (1974) 227–255.
[9] M.G. Worster, Convective flow problems in geological fluid dynamics, 1983, Ph.D. thesis, University of Cambridge.
[10] J.S. Wettlaufer, M.G. Worster, H.E. Huppert, Solidification of leads: theory, experiment, and field observations, J. Geophys. Res. 105 (2000) 1123–1134.
[11] J.S. Wettlaufer, M.G. Worster, H.E. Huppert, Natural convection during solidification of an alloy from above with application to the evolution of sea ice, J. Fluid. Mech. 344 (1997) 291–316.